Journal of Applied Fluid Mechanics, Vol. 8, No. 4, pp. 767-779, 2015.
Available online at www.jafmonline.net, ISSN 1735-3572, EISSN 1735-3645.
DOI: 10.18869/acadpub.jafm.67.223.22918

Unsteady Hydromagnetic Natural Convection Flow of a Heat Absorbing Fluid within a Rotating Vertical Channel in Porous Medium with Hall Effects

G. S. Seth†, B. Kumbhakar and R. Sharma

Department of Applied Mathematics, Indian School of Mines, Dhanbad-826004, INDIA

†Corresponding Author Email: *gsseth_ism@yahoo.com*

(Received April 19, 2014; accepted October 5, 2014)

ABSTRACT

Unsteady hydromagnetic natural convection flow of a viscous, incompressible, electrically conducting and temperature dependent heat absorbing fluid confined within a parallel plate rotating vertical channel in porous medium is investigated. Fluid flow within the channel is induced due to impulsive movement of one of the plates of the channel. Exact solution for the governing equations for fluid velocity and fluid temperature are obtained by Laplace transform technique. The expressions for the shear stress at the moving plate due to primary and secondary flows and those of rate of heat transfer at the moving and stationary plates are also derived. In order to gain some physical insight into the flow pattern, asymptotic behavior of the solution for fluid velocity and fluid temperature are analyzed for small and large values of time. The numerical values of primary and secondary fluid velocities and fluid temperature are displayed graphically whereas those of shear stress at the moving plate and rate of heat transfer at both the moving and stationary plates are presented in tabular form for various values of pertinent flow parameters.

Keywords: Hydromagnetic natural convection; Hall current; Rotation; Heat absorption; Porous medium.

NOMENCLATURE

B_0	uniform magnetic field
c_p	specific heat at constant pressure
g	acceleration due to gravity
G_r	Thermal Grashof number
h	distance between the plates
k_T	thermal conductivity of the fluid
K_1'	permeability of porous medium
K_1	permeability parameter
K^2	rotation parameter
m	Hall current parameter
M^2	magnetic parameter
p	fluid pressure
P_r	Prandtl number
Q_0	heat absorption coefficient
t'	time
T'	fluid temperature
U_0	characteristic velocity
u'	fluid velocity in x-direction
w'	fluid velocity in z-direction
β'	coefficient of thermal expansion
Ω	uniform angular velocity
σ	electrical conductivity
ρ	fluid density
ν	kinematic coefficient of viscosity
ω_e	cyclotron frequency
τ_e	electron collision time
φ	heat absorption parameter

1. INTRODUCTION

Natural convection flow in a vertical channel is investigated extensively in the past due to its varied and wide applications in science and engineering, namely, design of passive solar system for energy conversion, design of heat exchanger using liquid metal coolants, chemical devices, cooling of nuclear reactors, cooling of electronic equipments, geothermal reservoirs etc. Keeping in view this fact, several researchers, namely, Greif *et al*. (1971), Miyatake and Fujii (1972), Aung (1972), Kim *et al*. (1990), Lee and Yan (1994) and Campo *et al*. (2006) investigated natural convection flow in a vertical channel under different conditions whereas

Haddad (1999), Weidman and Medina (2008), Jana *et al*. (2011) and Das *et al*. (2011) studied natural convection flow through a fluid saturated porous medium within a vertical channel considering different aspects of the problem.

Theoretical/experimental investigation of unsteady natural convection flow of a viscous and incompressible fluid within a vertical channel is of great importance because transient fluid flow is expected at the start-up time of so many engineering devices, namely, generators, accelerators, flow meters, pumps, nuclear reactors etc. Taking into account this fact, several researchers investigated transient natural convection flow of a viscous and incompressible fluid in a parallel plate vertical channel under different initial and boundary conditions. Mention may be made of the research studies of Singh (1988), Joshi (1988), Paul *et al*. (1996), Singh *et al*. (1996) and Mandal *et al*. (2012). Recently, Jana *et al*. (2014) investigated oscillatory mixed convection flow of a viscous and incompressible fluid in a porous medium between two infinitely long vertical walls heated asymmetrically. In their study, oscillatory free and forced convection are generated by time varying gravitational field and applied periodic pressure gradient respectively.

Investigation of the problems of hydromagnetic flow with and without heat transfer in porous and non-porous media assumes significance due to its applications in various areas of science and technology such as MHD generator flow which includes disk systems (Yamasaki *et al*., 1988), magneto-thermo-acoustic generators (Vogin and Alemany, 2007), solar pond MHD generators (Kabakov and Yantovsky, 1993), hypersonic ionized boundary layers (Macheret *et al*., 2004), liquid metal processing (Bég *et al*., 2009), particle deposition in electrically conducting systems (Zueco *et al*., 2009), metallurgy, chemical and petroleum industries etc.

Keeping in view this fact, several researchers investigated hydromagnetic natural convection flow in a vertical channel considering different aspects of the problem. Mention may be made of the research studies of Yu (1965), Gupta and Gupta (1974), Datta and Jana (1976), Meric (1977) and Jha (2001).

Unsteady hydromagnetic Couette flow in a rotating environment has varied and wide applications in geophysics, astrophysics and in so many areas of fluid engineering viz. rotating hydromagnetic generators, vortex type MHD power generators, turbo machines, material processing etc. Keeping in view this fact Seth *et al*. (1982, 2011), Chandran *et al*. (1993), Singh *et al*. (1994), Hayat *et al*. (2004a, 2004b, 2004c), Das *et al*. (2009) and Sarkar *et al*. (2012) investigated unsteady hydromagnetic Couette flow of a viscous, incompressible and electrically conducting fluid in a rotating system considering various aspects of the problem. Ghosh *et al*. (2013) studied oscillatory hydromagnetic free and forced convection flow of a viscous, incompressible and electrically conducting fluid in a rotating channel in the presence of oblique magnetic field.

It is well known that in an ionized fluid, where density is low and/or magnetic field is strong, the effects of Hall current become significant as mentioned by Cowling (1957). Also, both Hall current and rotation induce secondary flow in the flow-field. Therefore, it seems to be significant to compare and contrast the effects of these two agencies and also to study their combined effects on the flow-field. Hall effects on fluid flow find applications in MHD power generation, MHD accelerators, nuclear power reactors, MHD pumps, underground energy storage system etc. Taking into account this fact, Jana and Datta (1980), Ghosh (2002), Ghosh and Pop (2004), Singh and Kumar (2010), Guchhait *et al*. (2011), Seth and Singh (2013), Seth *et al*. (2012), Jha and Apere (2012), Chauhan and Rastogi (2012) and Chauhan and Agrawal (2012) studied effects of Hall current on MHD Couette flow in a rotating system considering different physical aspects of the problem.

It is observed that there is considerable temperature difference between the surface of the solid and ambient fluid in so many fluid flow problems of physical interest. This prompted many researchers to consider temperature dependent heat source and/or sink which may have strong influence on heat transfer characteristics. The research studies related to convective flow of heat generating and/or absorbing fluid is of much significance in several physical problems, namely, convection in Earth's mantle (McKenzie *et al*., 1974), post accident heat removal (Baker et al., 1976), fluids undergoing exothermic and/or endothermic chemical reaction (Vajrvelu and Nayfeh, 1992), fire and combustion modeling (Delichatsios, 1988), development of metal waste from spent nuclear fuel (Westphal *et al*., 1994), applications in the field of nuclear energy (Crepeau and Clarksean, 1997) etc. Taking into consideration this fact Jha (2003) and Jha and Ajibade (2009, 2010) investigated transient free convective flow of heat generating/absorbing fluid within a vertical channel considering different aspects of the problem.

Aim of the present investigation is to study unsteady hydromagnetic natural convection Couette flow with Hall effects of a viscous, incompressible, electrically conducting and temperature dependent heat absorbing fluid through a uniform porous medium confined within a rotating vertical channel in the presence of uniform transverse magnetic field. Fluid flow within the channel is induced due to impulsive movement of one of the plates of the channel. Fluids as well as channel rotate in unison with uniform angular velocity about an axis normal to the planes of the plates of the channel. This study may have applications in science and engineering, namely, thermo-nuclear engineering, geophysical and astrophysical fluid dynamics, geothermal power extraction, plasma aerodynamics, extraction of oil and gases from reservoirs, MHD power generation and manufacturing processes.

2. FORMULATION OF THE PROBLEM AND ITS SOLUTION

Consider unsteady natural convection flow of a viscous, incompressible and electrically conducting heat absorbing fluid confined within parallel vertical plates $y=0$ and $y=h$ of infinite extent in x and z directions. x –axis is taken in upward direction along one of the plates and y–axis is normal to the planes of the plates. The channel is filled with a homogeneous porous material and the porous medium is saturated with heat absorbing fluid. A uniform transverse magnetic field B_0 is applied in a direction which is parallel to y –axis. The fluid and channel rotate in unison with uniform angular velocity Ω about y –axis. Initially (*i.e.*, at time $t' \le 0$), fluid and plates of the channel are assumed to be at rest and at uniform temperature T_h. At time $t'>0$, the plate $y=0$ starts moving with uniform velocity U_0 in x–direction and its temperature is raised or reduced to T_w while the plate $y=h$ is kept fixed and is maintained at T_h. Figure 1 shows the geometrical configuration of the problem.

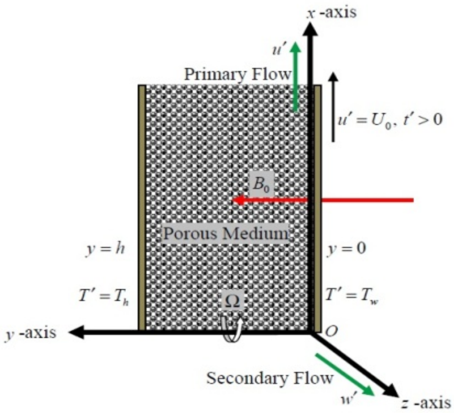

Fig. 1. Geometry of the problem.

It is assumed that no external electric field is applied in the flow-field so that the effect of polarization of fluid is neglected *i.e.*, electric field $\vec{E}=(0,0,0)$. The induced magnetic field produced by fluid motion is neglected in comparison to the applied one. This is justified because magnetic Reynolds number is very small for liquid metals and partially ionized fluids which are used in industrial processes (Cramer and Pai, 1973). Since plates of the channel are of infinite extent in x and z directions and are electrically non-conducting, all the physical quantities except pressure depend on y and t' only.

Thus, the equation of continuity $\nabla.\vec{q}=0$ and solenoidal relation for magnetic field $\nabla.\vec{B}=0$ imply that

$$\vec{q}=(u',0,w') \text{ and } \vec{B}=(0,B_0,0), \tag{1}$$

where u' and w' are fluid velocities in x and z directions respectively.

With the assumptions made above, the governing equations for unsteady hydromagnetic natural convection flow of a viscous, incompressible and electrically conducting heat absorbing fluid with Hall effects in a rotating system, under Boussinesq approximation, are given by

$$\frac{\partial u'}{\partial t'}+2\Omega w'=\nu\frac{\partial^2 u'}{\partial y^2}-\left(\frac{\sigma B_0^2}{\rho}\right)\frac{(u'+mw')}{(1+m^2)}-\frac{\nu}{K_1'}u' +g\beta'(T'-T_h), \tag{2}$$

$$\frac{\partial w'}{\partial t'}-2\Omega u'=\nu\frac{\partial^2 w'}{\partial y^2}+\left(\frac{\sigma B_0^2}{\rho}\right)\frac{(mu'-w')}{(1+m^2)}-\frac{\nu}{K_1'}w', \tag{3}$$

$$0=-\frac{1}{\rho}\frac{\partial p}{\partial y}, \tag{4}$$

$$\rho c_p\frac{\partial T'}{\partial t'}=k_T\frac{\partial^2 T'}{\partial y^2}-Q_0(T'-T_h), \tag{5}$$

where ν, σ, ρ, K_1', g, β', T', $m=\omega_e\tau_e$, ω_e, τ_e, k_T, C_p, Q_0 and p are, respectively, kinematic coefficient of viscosity, electrical conductivity, fluid density, permeability of porous medium, acceleration due to gravity, coefficient of thermal expansion, fluid temperature, Hall current parameter, cyclotron frequency, electron collision time, thermal conductivity, specific heat at constant pressure, heat absorption coefficient and fluid pressure including centrifugal force.

Initial and boundary conditions for the fluid flow problem are specified as

$$t'\le 0: \quad u'=w'=0,\ T'=T_h \text{ at } 0\le y\le h, \tag{6a}$$

$$t'>0: \quad u'=U_0,\ w'=0,\ T'=T_w \text{ at } y=0, \tag{6b}$$

$$u'=w'=0,\ T'=T_h \text{ at } y=h. \tag{6c}$$

In order to non-dimensionalize Eqs. (2), (3) and (5), we introduce the following non-dimensional variables and parameters:

$$\left.\begin{array}{l} \eta=y/h,\ u=u'/U_0,\ w=w'/U_0,\ t=\nu t'/h^2, \\ T=\left(T'-T_h\right)/\left(T_w-T_h\right),\ G_r=g\beta'\left(T_w-T_h\right)h^2/\nu U_0, \\ K_1=K_1'/h^2,\ K^2=\Omega h^2/\nu,\ M^2=\sigma B_0^2h^2/\rho\nu, \\ P_r=\nu\rho C_p/k_T,\ \varphi=Q_0h^2/\nu\rho C_p, \end{array}\right\} \tag{7}$$

where G_r, K_1, K^2, M^2, P_r and φ are, respectively, thermal Grashof number, permeability parameter, rotation parameter (reciprocal of Ekman number), magnetic parameter (square of Hartman number), Prandtl number and heat absorption parameter.

With the help of (7), Eqs. (2), (3) and (5), in non-dimensional form, assume the following form:

$$\frac{\partial u}{\partial t}+2K^2w=\frac{\partial^2 u}{\partial\eta^2}-\frac{M^2(u+mw)}{\left(1+m^2\right)}-\frac{u}{K_1}+G_rT, \tag{8}$$

$$\frac{\partial w}{\partial t}-2K^2u=\frac{\partial^2 w}{\partial \eta^2}+\frac{M^2\left(mu-w\right)}{\left(1+m^2\right)}-\frac{w}{K_1}, \tag{9}$$

$$\frac{\partial T}{\partial t}=\frac{1}{P_r}\frac{\partial^2 T}{\partial \eta^2}-\phi T. \tag{10}$$

Initial and boundary conditions (6a)-(6c), in non-dimensional form, are given by

$$t\le 0:\quad u=w=0,\ T=0 \text{ at } 0\le\eta\le 1, \tag{11a}$$
$$t>0:\quad u=1,\ w=0,\ T=1 \text{ at } \eta=0, \tag{11b}$$
$$u=w=0,\ T=0 \text{ at } \eta=1. \tag{11c}$$

Equations (8) and (9) are combined and expressed in compact form which is given below:

$$\frac{\partial F}{\partial t}+\lambda_1 F=\frac{\partial^2 F}{\partial \eta^2}+G_r T \tag{12}$$

where

$$\left.\begin{aligned} &F=u+iw,\ \lambda_1=m_1-im_2,\\ &m_1=M^2/(1+m^2)+(1/K_1),\\ &m_2=mM^2/(1+m^2)+2K^2.\end{aligned}\right\} \tag{13}$$

Initial and boundary conditions (11a)-(11c), in compact form, are given by

$$t\le 0:\quad F=0,\ T=0 \text{ at } 0\le\eta\le 1, \tag{14a}$$
$$t>0:\quad F=1,\ T=1 \text{ at } \eta=0, \tag{14b}$$
$$F=0,\ T=0 \text{ at } \eta=1. \tag{14c}$$

Exact solution for fluid temperature $T(\eta,t)$ and fluid velocity $F(\eta,t)$ is obtained by Laplace transform technique and is expressed in the following form after simplification,

$$\begin{aligned} T(\eta,t)=\frac{1}{2}\sum_{k=0}^{\infty}\Big[&e^{\alpha_1}erfc\left(\beta_1+\gamma_1\right)+e^{-\alpha_1}erfc\left(\beta_1-\gamma_1\right)\\ &-e^{\alpha_2}erfc\left(\beta_2+\gamma_1\right)-e^{-\alpha_2}erfc\left(\beta_2-\gamma_1\right)\Big], \end{aligned} \tag{15}$$

$$F(\eta,t)=\frac{1}{2}\sum_{k=0}^{\infty}\left[F_1(\eta,t)-\frac{G_r^*}{\lambda_2}\left\{F_2(\eta,t)-F_3(\eta,t)\right\}\right], \tag{16}$$

where

$$G_r^*=G_r/(1-P_r),\ \ \lambda_2=(P_r\varphi-\lambda_1)/(1-P_r),$$

$$\begin{aligned} F_1(\eta,t)=&e^{\alpha_3}erfc\left(\beta_3+\gamma_2\right)+e^{-\alpha_3}erfc\left(\beta_3-\gamma_2\right)\\ &-e^{\alpha_4}erfc\left(\beta_4+\gamma_2\right)-e^{-\alpha_4}erfc\left(\beta_4-\gamma_2\right),\end{aligned}$$

$$\begin{aligned} F_2(\eta,t)=e^{\delta_0}\Big\{&e^{\alpha_5}erfc\left(\beta_3+\gamma_3\right)+e^{-\alpha_5}erfc\left(\beta_3-\gamma_3\right)\\ &-e^{\alpha_6}erfc\left(\beta_4+\gamma_3\right)-e^{-\alpha_6}erfc\left(\beta_4-\gamma_3\right)\Big\}\\ &-e^{\alpha_3}erfc\left(\beta_3+\gamma_2\right)-e^{-\alpha_3}erfc\left(\beta_3-\gamma_2\right)\\ &+e^{\alpha_4}erfc\left(\beta_4+\gamma_2\right)+e^{-\alpha_4}erfc\left(\beta_4-\gamma_2\right),\end{aligned}$$

$$\begin{aligned} F_3(\eta,t)=e^{\delta_0}\Big\{&e^{\alpha_7}erfc\left(\beta_1+\gamma_4\right)+e^{-\alpha_7}erfc\left(\beta_1-\gamma_4\right)\\ &-e^{\alpha_8}erfc\left(\beta_2+\gamma_4\right)-e^{-\alpha_8}erfc\left(\beta_2-\gamma_4\right)\Big\}\\ &-e^{\alpha_1}erfc\left(\beta_1+\gamma_1\right)-e^{-\alpha_1}erfc\left(\beta_1-\gamma_1\right)\\ &+e^{\alpha_2}erfc\left(\beta_2+\gamma_1\right)+e^{-\alpha_2}erfc\left(\beta_2-\gamma_1\right),\end{aligned}$$

$$\delta_0=\lambda_2 t.$$

Expressions for $\alpha_i\,(i=1,2,...,8)$, $\beta_i\,(i=1,2,...,4)$, and $\gamma_i\,(i=1,2,...,4)$ are provided in Appendix I.

3. SOLUTION IN CASE OF UNIT PRANDTL NUMBER

It is noticed that the solution (16) for fluid velocity is not valid for fluids with unit Prandtl number. Since Prandtl number P_r is a measure of the relative strength of momentum diffusivity to thermal diffusivity of the fluid, fluid flow problem with $P_r=1$ corresponds to those fluids for which thicknesses of both the momentum and thermal boundary layers are of same order of magnitude. There are some fluids of physical interest which belong to this category (Cebeci, 2002). Substituting $P_r=1$ in Eq. (10) and following the same procedure as adopted in above analysis, exact solution for fluid temperature $T(\eta,t)$ and fluid velocity $F(\eta,t)$ is obtained and presented below:

$$\begin{aligned} T(\eta,t)=\frac{1}{2}\sum_{k=0}^{\infty}\Big[&e^{a\sqrt{\varphi}}erfc\left(\beta_3+\gamma_1\right)+e^{-a\sqrt{\varphi}}erfc\left(\beta_3-\gamma_1\right)\\ &-e^{b\sqrt{\varphi}}erfc\left(\beta_4+\gamma_1\right)-e^{-b\sqrt{\varphi}}erfc\left(\beta_4-\gamma_1\right)\Big], \end{aligned} \tag{17}$$

$$F(\eta,t)=\frac{1}{2}\sum_{k=0}^{\infty}\left[\left(1-\lambda_3\right)G_1\left(\eta,t\right)+\lambda_3 G_2\left(\eta,t\right)\right], \tag{18}$$

where

$$\lambda_3=G_r/(\lambda_1-\varphi),$$

$$\begin{aligned} G_1(\eta,t)=&e^{\alpha_3}erfc\left(\beta_3+\gamma_1\right)+e^{-\alpha_3}erfc\left(\beta_3-\gamma_1\right)\\ &-e^{\alpha_4}erfc\left(\beta_4+\gamma_1\right)-e^{-\alpha_4}erfc\left(\beta_4-\gamma_1\right),\end{aligned}$$

$$\begin{aligned} G_2(\eta,t)=&e^{a\sqrt{\varphi}}erfc\left(\beta_3+\gamma_1\right)+e^{-a\sqrt{\varphi}}erfc\left(\beta_3-\gamma_1\right)\\ &-e^{b\sqrt{\varphi}}erfc\left(\beta_4+\gamma_1\right)-e^{-b\sqrt{\varphi}}erfc\left(\beta_4-\gamma_1\right).\end{aligned}$$

4. SHEAR STRESS AT THE MOVING PLATE

The expressions for shear stress τ_x due to primary flow and shear stress τ_z due to secondary flow at the moving plate $\eta=0$ are presented in the following form.

$$\tau_x+i\tau_z=\frac{1}{2}\sum_{k=0}^{\infty}\left[\tau_1(k)-\frac{G_r^*}{\lambda_2}\left\{\tau_2(k)-\tau_3(k)\right\}\right], \tag{19}$$

where

$$\begin{aligned} \tau_1(k)=&\sqrt{\lambda_1}\left[\theta_1(k)-\theta_2(k)+\theta_1(k+1)-\theta_2(k+1)\right]\\ &-\frac{2}{\sqrt{\pi t}}\left[\psi_1(k)+\psi_1(k+1)\right],\end{aligned}$$

$$\begin{aligned} \tau_2(k)=e^{\delta_0}&\sqrt{\left(\lambda_1+\lambda_2\right)}\left[\theta_3(k)-\theta_4(k)+\theta_3(k+1)\right.\\ &\left.-\theta_4(k+1)\right]-\frac{2e^{\delta_0}}{\sqrt{\pi t}}\left[\psi_2(k)+\psi_2(k+1)\right]\\ &-\sqrt{\lambda_1}\left[\theta_1(k)-\theta_2(k)+\theta_1(k+1)-\theta_2(k+1)\right]\\ &+\frac{2}{\sqrt{\pi t}}\left[\psi_1(k)+\psi_1(k+1)\right],\end{aligned}$$

$$\tau_3(k) = e^{\delta_0}\sqrt{P_r(\varphi+\lambda_2)}\big[\theta_5(k)-\theta_6(k)+\theta_5(k+1)$$
$$-\theta_6(k+1)\big]-2e^{\delta_0}\sqrt{P_r/\pi t}\big[\psi_3(k)+\psi_3(k+1)\big]$$
$$-\sqrt{P_r\varphi}\big[\theta_7(k)-\theta_8(k)+\theta_7(k+1)-\theta_8(k+1)\big]$$
$$+2\sqrt{P_r/\pi t}\big[\psi_4(k)+\psi_4(k+1)\big].$$

Expressions for $\theta_i(k)(i=1,2,...,8)$ and $\psi_i(k)(i=1,2,...,4)$ are prescribed in Appendix II.

5. RATE OF HEAT TRANSFER AT THE PLATES

The expressions for rate of heat transfer at the moving plate $\eta=0$ *i.e.*, $\left(\dfrac{\partial T}{\partial \eta}\right)_{\eta=0}$ and rate of heat transfer at the stationary plate $\eta=1$ *i.e.*, $\left(\dfrac{\partial T}{\partial \eta}\right)_{\eta=1}$ are presented below:

$$\left(\frac{\partial T}{\partial \eta}\right)_{\eta=0} = \frac{1}{2}\sum_{k=0}^{\infty}\Big[\sqrt{P_r\varphi}\,\{\theta_7(k)-\theta_8(k)+\theta_7(k+1)$$
$$-\theta_8(k+1)\}-2\sqrt{P_r/\pi t}\,\{\psi_4(k)+\psi_4(k+1)\}\Big], \tag{20}$$

$$\left(\frac{\partial T}{\partial \eta}\right)_{\eta=1} = \frac{1}{2}\sum_{k=0}^{\infty}\Big[2\sqrt{\mathrm{P}_r/\pi t}\,\psi_4(2k+1)$$
$$-\sqrt{\mathrm{P}_r\,\phi}\,\{\theta_7(k+1/2)-\theta_8(k+1/2)\}\Big]. \tag{21}$$

6. ASYMPTOTIC BEHAVIOR OF THE SOLUTION

We shall now discuss asymptotic behavior of the solution (15) and (16) for small as well as large values of time *t* to gain some physical insight into the flow pattern.

6.1 Case-I: When Time *t* is Small (*i.e.* *t* << 1)

The expressions for fluid temperature $T(\eta,t)$, primary fluid velocity $u(\eta,t)$ and secondary fluid velocity $w(\eta,t)$, which are obtained from the analytical solution (15) and (16) for small values of time *t*, are given by

$$T(\eta,t)=\sum_{k=0}^{\infty}\Big[\big\{erfc(\beta_1)-erfc(\beta_2)\big\}$$
$$+(P_r\varphi/2)\big\{a^2erfc(\beta_1)-b^2erfc(\beta_2)\big\}$$
$$-\varphi\sqrt{P_rt/\pi}\left(a\,e^{-\beta_1^2}-b\,e^{-\beta_2^2}\right)\Big], \tag{22}$$

$$u(\eta,t)=\sum_{k=0}^{\infty}\Big[\left(1-G_r^*t\right)\big\{erfc(\beta_3)-erfc(\beta_4)\big\}$$
$$+\left\{\left(1-G_r^*t/2\right)m_1-(1+m_5t)G_r^*/2\right\}$$
$$\times\left\{a^2\,erfc(\beta_3)-b^2\,erfc(\beta_4)\right\}$$
$$-\sqrt{t/\pi}\left\{\left(1+2G_r^*t/3\right)m_1+G_r^*\left(1+5m_5t/6\right)\right\}$$
$$\times\left(a\,e^{-\beta_3^2}-b\,e^{-\beta_4^2}\right)+\left(G_r^*/6\right)\sqrt{t/\pi}\,(m_1-m_5/2)$$
$$\times\left(a^3\,e^{-\beta_3^2}-b^3\,e^{-\beta_4^2}\right)-\left(G_r^*/4\right)(m_1/3+m_5/2)$$
$$\times\left\{a^4\,erfc(\beta_3)-b^4\,erfc(\beta_4)\right\}$$
$$+G_r^*\Big[t\left\{erfc(\beta_1)-erfc(\beta_2)\right\}$$
$$+(P_r/2)(1+\varphi t+m_5t)\left\{a^2\,erfc(\beta_1)-b^2\,erfc(\beta_2)\right\}$$
$$+(\varphi/3+m_5/2)\left(P_r^2/4\right)\left\{a^4\,erfc(\beta_1)-b^4\,erfc(\beta_2)\right\}$$
$$-\sqrt{P_rt/\pi}\,(1+2\varphi t/3+5m_5t/6)$$
$$\times\left(a\,e^{-\beta_1^2}-b\,e^{-\beta_2^2}\right)-(P_r/6)\sqrt{P_rt/\pi}\,(\varphi+m_5/2)$$
$$\times\left(a^3\,e^{-\beta_1^2}-b^3\,e^{-\beta_2^2}\right)\Big]\Big], \tag{23}$$

$$w(\eta,t)=\sum_{k=0}^{\infty}\Big[\sqrt{t/\pi}\left\{\left(1-2G_r^*t/3\right)m_2-5G_r^*m_6t/6\right\}$$
$$\times\left(a\,e^{-\beta_3^2}-b\,e^{-\beta_4^2}\right)-\left(G_r^*/6\right)\sqrt{t/\pi}\,(m_2+m_6/2)$$
$$\times\left(a^3\,e^{-\beta_3^2}-b^3\,e^{-\beta_4^2}\right)-(1/2)\left\{\left(1-G_r^*t\right)m_2-G_r^*m_6t\right\}$$
$$\times\left\{a^2\,erfc(\beta_3)-b^2\,erfc(\beta_4)\right\}$$
$$+\left(G_r^*/4\right)(m_2/3+m_6/2)$$
$$\times\left\{a^4\,erfc(\beta_3)-b^4\,erfc(\beta_4)\right\}$$
$$+G_r^*\Big[(5m_6t/6)\sqrt{P_rt/\pi}\left(a\,e^{-\beta_1^2}-b\,e^{-\beta_2^2}\right)$$
$$+(P_rm_6/12)\sqrt{P_rt/\pi}\left(a^3\,e^{-\beta_1^2}-b^3\,e^{-\beta_2^2}\right)$$
$$-(P_rm_6t/2)\left\{a^2\,erfc(\beta_1)-b^2\,erfc(\beta_2)\right\}$$
$$-\left(m_6P_r^2/8\right)\left\{a^4\,erfc(\beta_1)-b^4\,erfc(\beta_2)\right\}\Big]\Big], \tag{24}$$

where
$m_3=P_r(\varphi-m_1)/(1-P_r),\ m_4=m_2P_r/(1-P_r),$
$m_5=(m_1-\varphi P_r)/(1-P_r),\ m_6=m_2/(1-P_r).$

It is evident from the expressions (22) to (24) that for small values of time *t*, *i.e.* at the initial stage, there arise double boundary layers of thicknesses $O\left(\sqrt{t}\right)$ and $O\left(\sqrt{t/P_r}\right)$ adjacent to the moving plate $\eta=0$ due to initial impulsive movement of the plate. The boundary layer of thickness $O\left(\sqrt{t}\right)$ may be identified as classical Rayleigh boundary layer whereas boundary layer of thickness $O\left(\sqrt{t/P_r}\right)$ may be recognized as modified Rayleigh boundary layer which may be viewed as classical Rayleigh boundary layer modified by thermal diffusion. The fluid temperature $T(\eta,t)$ is considerably affected by thermal diffusion and heat absorption. The primary velocity $u(\eta,t)$ is independent of rotation whereas secondary fluid velocity $w(\eta,t)$ is unaffected by permeability of the medium and heat absorption. However, both the primary and secondary fluid velocities are considerably affected by magnetic field, Hall current, thermal buoyancy force and thermal diffusion. In the absence of Hall current, *i.e.*, when $m=0$, secondary fluid velocity $w(\eta,t)$ is unaffected by magnetic field. Up to this stage, there are no inertial oscillations in the flow-field.

6.2 Case-II: When Time *t* is Large (*i.e. t* >>1)

The expressions for fluid temperature $T(\eta,t)$, primary fluid velocity $u(\eta,t)$ and secondary fluid velocity $w(\eta,t)$, which are obtained from the analytical solution (15) and (16) for large values of time *t*, are given by

$$T(\eta,t)=\frac{1}{2}\sum_{k=0}^{\infty}\Big[e^{-\varphi t}\left(\varphi_{13}-\varphi_{14}\right)+2\Big(e^{-a\sqrt{P_r\varphi}}-e^{-b\sqrt{P_r\varphi}}\Big)\Big], \tag{25}$$

$$u(\eta,t)=u_s(\eta)+u_t(\eta,t), \tag{26}$$

and $$w(\eta,t)=w_s(\eta)+w_t(\eta,t), \tag{27}$$

where

$$\begin{aligned}u_s=\sum_{k=0}^{\infty}\Big[&e^{-a\alpha}\left\{(1-m_8)\cos a\beta+m_9\sin a\beta\right\}\\&-e^{-b\alpha}\left\{(1-m_8)\cos b\beta+m_9\sin b\beta\right\}\\&+(m_8/2)\Big(e^{-a\sqrt{P_r\varphi}}-e^{-b\sqrt{P_r\varphi}}\Big)\Big],\end{aligned} \tag{28}$$

$$\begin{aligned}w_s=\sum_{k=0}^{\infty}\Big[&e^{-a\alpha}\left\{(1-m_8)\sin a\beta-m_9\cos a\beta\right\}\\&-e^{-b\alpha}\left\{(1-m_8)\sin b\beta-m_9\cos b\beta\right\}\\&+(m_9/2)\Big(e^{-a\sqrt{P_r\varphi}}-e^{-b\sqrt{P_r\varphi}}\Big)\Big],\end{aligned} \tag{29}$$

$$u_t(\eta,t)=u_{t_1}(\eta,t)+u_{t_2}(\eta,t), \tag{30}$$

$$\begin{aligned}u_{t_1}(\eta,t)=\frac{1}{2}\sum_{k=0}^{\infty}e^{-m_1t}\big[&(1-m_8)(\varphi_1-\varphi_3)-m_9(\varphi_2-\varphi_4)\\&+\{m_8\cos(m_6t)-m_9\sin(m_6t)\}(\varphi_9-\varphi_{11})\\&+\{m_8\sin(m_6t)+m_9\cos(m_6t)\}(\varphi_{10}-\varphi_{12})\big],\end{aligned} \tag{31}$$

$$\begin{aligned}u_{t_2}(\eta,t)=\frac{1}{2}\sum_{k=0}^{\infty}e^{-\varphi t}\big[&m_8(\varphi_{13}-\varphi_{14})\\&-\{m_8\cos(m_6t)-m_9\sin(m_6t)\}(\varphi_5-\varphi_7)\\&-\{m_8\sin(m_6t)+m_9\cos(m_6t)\}(\varphi_6-\varphi_8)\big],\end{aligned} \tag{32}$$

$$w_t(\eta,t)=w_{t_1}(\eta,t)+w_{t_2}(\eta,t), \tag{33}$$

$$\begin{aligned}w_{t_1}(\eta,t)=\frac{1}{2}\sum_{k=0}^{\infty}e^{-m_1t}\big[&(1-m_8)(\varphi_2-\varphi_4)-m_9(\varphi_1-\varphi_3)\\&+\{m_8\sin(m_6t)+m_9\cos(m_6t)\}(\varphi_9-\varphi_{11})\\&-\{m_8\cos(m_6t)-m_9\sin(m_6t)\}(\varphi_{10}-\varphi_{12})\big],\end{aligned} \tag{34}$$

$$\begin{aligned}w_{t_2}(\eta,t)=\frac{1}{2}\sum_{k=0}^{\infty}e^{-\varphi t}\big[&m_9(\varphi_{13}-\varphi_{14})\\&-\{m_8\sin(m_6t)+m_9\cos(m_6t)\}(\varphi_5-\varphi_7)\\&+\{m_8\cos(m_6t)-m_9\sin(m_6t)\}(\varphi_6-\varphi_8)\big],\end{aligned} \tag{35}$$

$$\left.\begin{aligned}&m_7=\varphi-m_5,\\&m_8=m_5G_r^*\big/(m_5^2+m_6^2),\\&m_9=m_6G_r^*\big/(m_5^2+m_6^2),\end{aligned}\right\} \tag{36}$$

$$\left.\begin{aligned}&\alpha=\frac{1}{\sqrt{2}}\left\{\left(m_1^2+m_2^2\right)^{1/2}+m_1\right\}^{1/2},\\&\beta=\frac{1}{\sqrt{2}}\left\{\left(m_1^2+m_2^2\right)^{1/2}-m_1\right\}^{1/2}.\end{aligned}\right\} \tag{37}$$

Expressions for $\varphi_i\ (i=1,2,...,14)$ are prescribed in Appendix III.

It is evident from the expression (25) that for large values of time *t*, fluid temperature $T(\eta,t)$ is in quasi-steady state. Steady state fluid temperature is confined within a boundary layer of thickness $O\left(\left(\sqrt{P_r\varphi}\right)^{-1}\right)$ which may be identifies as thermal boundary layer. The thickness of this boundary layer decreases on increasing either P_r or φ or both. For large values of time *t*, fluid temperature $T(\eta,t)$ approaches to steady state in the dimensionless time of $O\left(\varphi^{-1}\right)$. It is also noticed from expression (25) that there exist no inertial and spatial oscillations in the temperature field.

It is revealed from the expressions (26) and (27) that for large values of time *t*, flow-field is in quasi-steady state. Steady state flow, represented by $u_s(\eta)$ and $w_s(\eta)$, is confined within double boundary layer of thicknesses $O\left(\alpha^{-1}\right)$ and $O\left(\left(\sqrt{P_r\varphi}\right)^{-1}\right)$. The boundary layers of thickness $O\left(\alpha^{-1}\right)$ may be recognized as modified Ekman-Hartmann boundary layer. It is noticed from the expressions (13) and (37) that, α increases on increasing either K^2 or M^2 and decreases on increasing either m or K_1. Thus, we may conclude that the thickness of modified Ekman-Hartmann boundary layer decreases on increasing either K^2 or M^2 and it increases on increasing either m or K_1. It is also observed from (28) and (29) that steady state flow exhibits spatial oscillations in the flow-field excited by Hall current, magnetic field, rotation and permeability of the medium.

It is evident from expressions (30) to (35) that unsteady state flow, represented by $u_t(\eta,t)$ and $w_t(\eta,t)$ is divided into two regions, viz. region I and region II. Region I is described by $u_{t_1}(\eta,t)$ and $w_{t_1}(\eta,t)$ whereas region II is represented by $u_{t_2}(\eta,t)$ and $w_{t_2}(\eta,t)$. It is also revealed from expressions (30) to (35) that unsteady state flow exhibits inertial oscillations in the flow-field excited by Hall current, rotation and thermal diffusion. The inertial oscillations in the region I damp out effectively in dimensionless time of $O(m_1^{-1})$ whereas those in region II damp out effectively in dimensionless time of $O\left(\varphi^{-1}\right)$ when final steady state is developed. It is evident from (13) that m_1 increases on increasing M^2 and it decreases on increasing either m or K_1. This implies that, magnetic field tends to reduce time of decay of inertial oscillations in region I whereas Hall current and permeability of the medium have tendency to enhance time of decay of inertial oscillations in this region. Heat absorption tends to reduce time of decay of inertial oscillations in region II. In the absence of rotation, Hall current and thermal diffusion there are no inertial oscillations in the flow-field. This implies that, either rotation or Hall current or thermal diffusion or all of them together generate inertial oscillations in the flow-field for large values of time *t*.

7. RESULTS AND DISCUSSION

To highlight the influence of heat absorption and time on fluid temperature the numerical values of fluid temperature *T*, computed from the analytical solution (15), are displayed graphically versus channel width variable η in Figs. 2 and 3 for various values heat absorption parameter φ and time t taking Prandtl number $P_r = 0.71$ (ionized air). It is perceived from Figs. 2 and 3 that fluid temperature T decreases on increasing φ whereas it increases on increasing t. This implies that heat absorption has a tendency to reduce fluid temperature whereas fluid temperature is getting enhanced with the progress of time. It is worthy to note from Fig. 3 that fluid temperature T attains steady state when $t \geq 0.6$.

In order to analyze the effects of magnetic field, Hall current, rotation, permeability of the porous medium, thermal buoyancy force, heat absorption and time on the flow-field, numerical values of the primary fluid velocity *u* and secondary fluid velocity *w*, computed from the analytical solution (16), are depicted graphically versus channel width variable η in Figs. 4 to 10 for various values of magnetic parameter M^2, Hall current parameter m, rotation parameter K^2, permeability parameter K_1, thermal Grashof number G_r, heat absorption parameter φ and time t taking Prandtl number $P_r = 0.71$. Figure 4 describes the effect of magnetic field on the primary fluid velocity *u* and secondary fluid velocity *w*. It is revealed from Fig. 4 that *u* and *w* decrease on increasing M^2 which implies that magnetic field has retarding influence on the fluid flow in both the primary and secondary flow

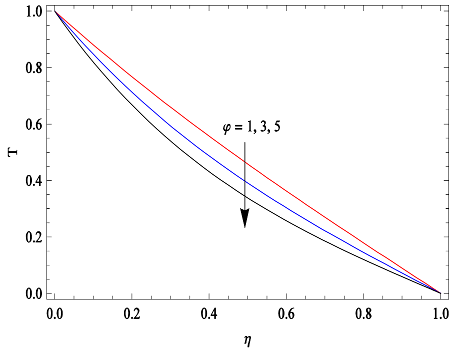

Fig. 2. Temperature profiles when t= 0.5.

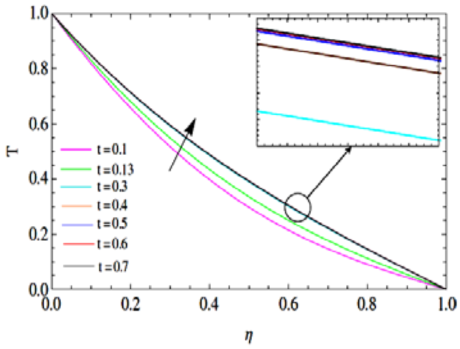

Fig. 3. Temperature profiles when φ = 3.

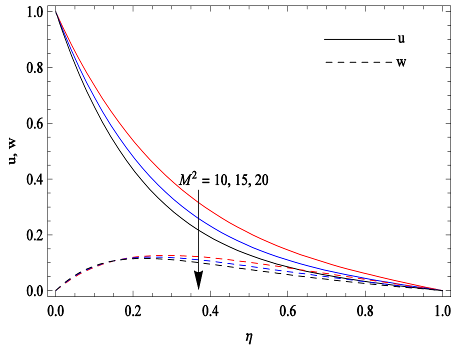

Fig. 4. Primary and secondary velocity profiles when $m = 0.5$, $K^2 = 2$, $K_1 = 0.2$, $G_r = 4$, $\varphi = 3$ and $t = 0.5$.

directions. This is due to the fact that the application of a magnetic field to an electrically conducting fluid gives rise to a force, called Lorentz force, which has the tendency to resist the fluid motion.Figure 5 depicts the influence of Hall current on the primary fluid velocity *u* and secondary fluid velocity *w*. It is evident from Fig. 5 that *u* and *w* increase on increasing m. It is widely known that, in an ionized fluid whose density is low and/or applied magnetic field is strong, Hall current appears in the flow-field which acts perpendicular to both electric and magnetic fields i.e. Hall current acts in the direction of primary flow and also it induces secondary flow in the flow-field. Keeping in view this fact, we may conclude that Hall current tends to accelerate fluid flow in both the primary and secondary flow directions. Figure 6 illustrates the effect of rotation on the primary fluid velocity *u* and secondary fluid velocity *w*. It is noticed from Fig. 6 that *u* decreases on increasing K^2 whereas *w* increases on increasing K^2.

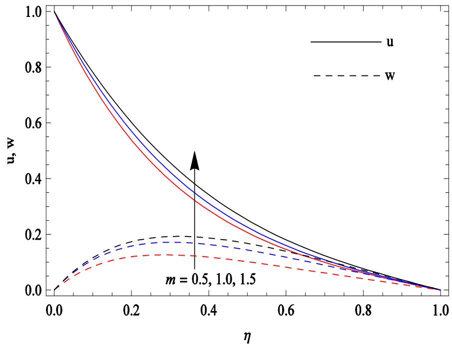

Fig. 5. Primary and secondary velocity profiles when M^2 = 10, K^2 =2, K_1 = 0.2, G_r = 4, φ = 3 and t = 0.5.

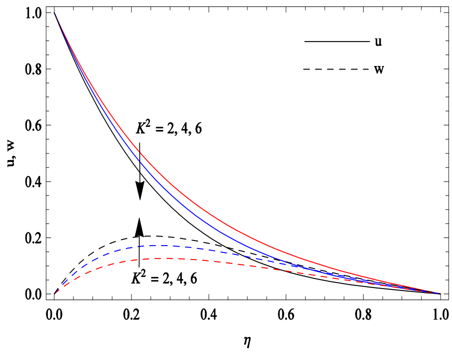

Fig. 6. Primary and secondary velocity profiles when M^2 = 10, m = 0.5, K_1 = 0.2, G_r = 4, φ = 3 and t = 0.5.

This implies that rotation tends to retard fluid flow in the primary flow direction whereas it has reverse effect on the fluid flow in the secondary flow direction. This is due to the fact that Coriolis force has a tendency to suppress fluid flow in the primary flow direction to generate fluid flow in the secondary flow direction.

Figure 7 demonstrates the effect of permeability of the porous medium on the primary fluid velocity u and secondary fluid velocity w. It is perceived from Fig. 7 that u and w increase on increasing K_1. This is due to the fact that an increase in permeability of resistance of the porosity of the medium which in turn accelerates the fluid flow in both the primary and secondary flow directions. Figure 8 shows the influence of thermal buoyancy force on the primary fluid velocity u and secondary fluid velocity w. It is observed from Fig. 8 that u and w increase on increasing G_r. Since G_r presents the relative strength of thermal buoyancy force to viscous force, an increase in thermal buoyancy force leads to an increase in G_r. This implies that thermal buoyancy force tends to accelerate fluid flow in both the primary and secondary flow directions. Figure 9 depicts the effects of heat absorption on the primary fluid velocity u and secondary fluid velocity w. It is noticed from Fig. 9 that u and w decrease on increasing φ

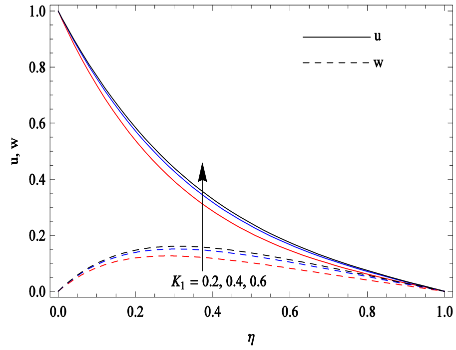

Fig. 7. Primary and secondary velocity profiles when M^2 = 10, m = 0.5, K^2 = 2, G_r = 4, φ = 3 and t = 0.5.

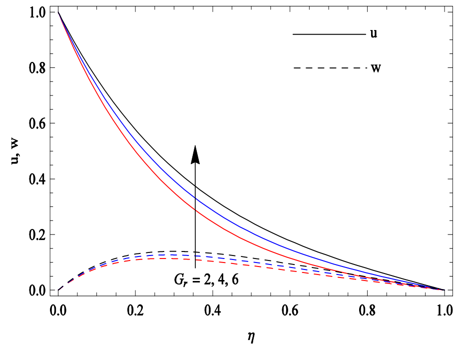

Fig. 8. Primary and secondary velocity profiles when M^2 = 10, m = 0.5, K^2 = 2, K_1 = 0.2, φ = 3 and t = 0.5.

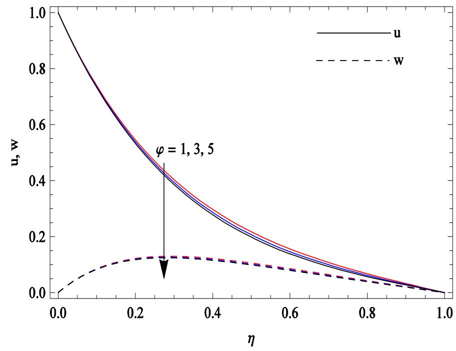

Fig. 9. Primary and secondary velocity profiles when M^2 = 10, m = 0.5, K^2 = 2, K_1 = 0.2, G_r = 4 and t = 0.5.

which implies that heat absorption has the tendency to retard fluid flow in both the primary and secondary flow directions. This is justified because fluid is becoming cooler due to heat absorption which is clearly evident from Fig. 2. Figure 10 demonstrates the effect of time t on the primary fluid velocity u and secondary fluid velocity w. It is evident from Fig. 10 that u and w increase on increasing t. This implies that fluid flow in both the primary and secondary flow directions is getting accelerated with the progress of time. It is evident from Eq. (8) that fluid velocity also depends on fluid temperature and fluid temperature is getting enhanced with the progress of time. Due to this reason fluid velocity is getting enhanced with the progress of time. It is interesting to note from Fig. 10 that the fluid flow in both the primary and secondary flow directions attains steady state when $t \geq 0.6$.

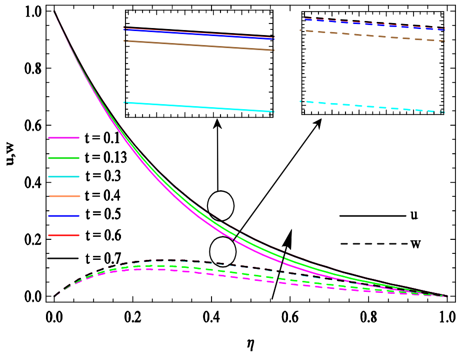

Fig. 10. Primary and secondary velocity profiles when M^2 = 10, m = 0.5, K^2 = 2, K_1 = 0.2, G_r = 4 and φ = 3.

The numerical values of shear stress at the moving plate $\eta = 0$ due to primary flow *i.e.*, τ_x and the shear stress at the moving plate $\eta = 0$ due to secondary flow *i.e.*, τ_z, computed from the analytical expression (19), are presented in tabular form in Tables 1 to 4 for various values of $M^2, m, K^2, G_r, K_1, \varphi$ and t whereas those of rate of heat transfer at the moving plate *i.e.*, $(\partial T/\partial \eta)_{\eta=0}$ and at the stationary plate *i.e.*, $(\partial T/\partial \eta)_{\eta=1}$, calculated from the analytical expressions (20) and (21), are provided in Table 5 for different values of φ and t taking $P_r = 0.71$.

Table 1 Shear stress at the moving plate when M = 0.5, K_1 = 0.2, G_r = 6, φ = 3 and t = 0.5

	$K^2 \rightarrow$ / $M^2 \downarrow$	2	4	6
$-\tau_x$	10	2.71554	2.92491	3.16575
	15	3.32803	3.62788	3.69657
	20	3.86330	4.01042	4.17698
τ_z	10	1.24210	1.77784	2.22581
	15	1.33815	1.80714	2.23045
	20	1.42618	1.84758	2.23605

It is evident from Table 1 that both the primary shear stress τ_x and secondary shear stress τ_z at the moving plate increase on increasing either M^2 or K^2. This implies that magnetic field and rotation tend to enhance both the primary and secondary shear stress at the moving plate. It is revealed from Table 2 that primary shear stress τ_x decreases whereas secondary shear stress τ_z increases on increasing m. This implies that Hall current tends to reduce primary shear stress at the moving plate whereas it has reverse effect on secondary shear stress at the moving plate.

Table 2 Shear stress at the moving plate when M^2 = 10, K_1 = 0.2, G_r = 6, φ = 3 and t = 0.5

	$K^2 \rightarrow$ / $m \downarrow$	2	4	6
$-\tau_x$	0.5	2.71554	2.92491	3.16575
	1.0	2.33287	2.61422	2.91097
	1.5	2.01010	2.34066	2.67768
τ_z	0.5	1.24210	1.77784	2.24581
	1.0	1.55333	2.09900	2.55743
	1.5	1.63136	2.20243	2.66718

It is observed from Table 3 that τ_x decreases whereas τ_z increases on increasing either G_r or K_1. This implies that, thermal buoyancy force and permeability of the medium tend to reduce primary shear stress at the moving plate whereas these agencies have reverse effect on secondary shear stress at the moving plate

Table 3 Shear stress at the moving plate when M^2 = 10, m = 0.5, K^2 = 4, φ = 3 and t = 0.5

	$K_1 \rightarrow$ / $G_r \downarrow$	0.2	0.5	0.8
$-\tau_x$	4	3.25474	2.88517	2.79067
	6	2.92491	2.54116	2.44305
	8	2.59508	2.19715	2.09544
τ_z	4	1.69529	1.87268	1.92389
	6	1.77784	1.97153	2.02755
	8	1.86040	2.07038	2.13122

It is noticed from Table 4 that τ_x increases and τ_z decreases on increasing φ whereas τ_x decreases and τ_z increases on increasing t. This implies that heat absorption tends to enhance primary shear stress at the moving plate whereas it has a reverse effect on secondary shear stress at the moving plate. As time progresses, primary shear stress at the moving plate is getting reduced whereas secondary shear stress at the moving plate is getting enhanced.

Table 4 Shear stress at the moving plate when M^2 = 10, m = 0.5, K^2 = 4, K_1 = 0.2 and G_r = 6

	$t \rightarrow$ / $\varphi \downarrow$	0.3	0.5	0.7
$-\tau_x$	1	2.87340	2.86937	2.86913
	3	2.92619	2.92491	2.92484
	5	2.97046	2.97041	2.97039
τ_z	1	1.79655	1.80338	1.80374
	3	1.77404	1.77784	1.77798
	5	1.75530	1.75732	1.75737

It is evident from Table 5 that rate of heat transfer at the moving plate *i.e.*, $(\partial T/\partial \eta)_{\eta=0}$ increases whereas rate of heat transfer at the stationary plate *i.e.*, $(\partial T/\partial \eta)_{\eta=1}$ decreases on increasing φ. $(\partial T/\partial \eta)_{\eta=0}$ decreases whereas $(\partial T/\partial \eta)_{\eta=1}$

increases on increasing t. This implies that heat absorption tends to enhance rate of heat transfer at the moving plate whereas it has a reverse effect on the rate of heat transfer at the stationary plate. As time progresses, rate of heat transfer at the moving plate is getting reduced whereas rate of heat transfer at the stationary plate is getting enhanced.

Table 5 Rate of heat transfer at the moving and stationary plates

	$t \rightarrow$ $\varphi \downarrow$	0.1	0.3	0.5
$-\left(\frac{\partial T}{\partial \eta}\right)_{\eta=0}$	1	1.65348	1.24752	1.22726
	3	1.93497	1.63638	1.62640
	5	2.19970	1.97829	1.97333
$-\left(\frac{\partial T}{\partial \eta}\right)_{\eta=1}$	1	0.47716	0.86943	0.88970
	3	0.41885	0.70663	0.71661
	5	0.36824	0.58109	0.58604

8. CONCLUSION

An investigation of unsteady hydromagnetic natural convection flow of a viscous, incompressible, electrically conducting and heat absorbing fluid within a parallel plate rotating vertical channel in porous medium is carried out. Significant findings of the problem are mentioned below:

- Magnetic field and heat absorption have retarding influence on the fluid flow in both the primary and secondary flow directions.
- Hall current, permeability of porous medium and thermal buoyancy force have tendency to accelerate fluid flow in both the primary and secondary flow directions.
- Rotation tends to retard fluid flow in the primary flow direction whereas it has reverse effect on the fluid flow in the secondary flow direction.
- Fluid flow in both the primary and secondary flow directions is getting accelerated with the progress of time. It is interesting to note that fluid flow in both the primary and secondary flow directions attain steady state when $t \geq 0.6$.
- Heat absorption has tendency to reduce fluid temperature whereas fluid temperature is getting enhanced with the progress of time. Fluid temperature attains steady state when $t \geq 0.6$.
- Magnetic field and rotation have the tendency to enhance both the primary and secondary shear stress at the moving plate.
- Hall current, permeability of porous medium and thermal buoyancy force tend to reduce primary shear stress at the moving plate whereas these agencies have reverse effect on the secondary shear stress at the moving plate.
- Heat absorption tends to enhance both the primary shear stress and rate of heat transfer at the moving plate whereas it has a reverse effect on the secondary shear stress at the moving plate and rate of heat transfer at the stationary plate.
- As time progresses, primary shear stress at the moving plate and rate of heat transfer at the moving plate are getting reduced whereas secondary shear stress at the moving plate and rate of heat transfer at the stationary plate are getting enhanced.

ACKNOWLEDGEMENTS

Authors are grateful to Indian School of Mines, Dhanbad for providing financial support and good research facility to carry out this work.

REFERENCES

Aung, W. (1972). Fully Developed Laminar Free Convection between Vertical Plates Heated Asymmetrically. *Int. J. Heat Mass Transfer* 15(8), 1577-1580.

Baker, L., R. E. Faw and F. A. Kulacki (1976). Post-accident Heat Removal Part-I: Heat Transfer within an Internally Heated, Nonboiling Liquid Layer. *J. Nucl. Sci. Eng.*, 61 222-230.

Bég, O. A., A. Y. Bakier, V. R. Prasad, J. Zueco, and S. K. Ghosh (2009). Nonsimilar, Laminar, Steady, Electrically-Conducting Forced Convection Liquid Metal Boundary Layer Flow with Induced Magnetic Field Effects. *Int. J. Therm. Sci.* 48(8), 1596-1606.

Campo, A., O. Manca and B. Morrone (2006). Numerical Investigation of the Natural Convection Flows for Low-Prandtl Fluids in Vertical Parallel-Plates Channels. *J. Appl. Mech.* 73(1), 99-107.

Cebeci, T. (2002). *Convective Heat Transfer*, Horizons Publishing Inc., Long Beach, California.

Chandran, P., N. C. Sacheti and A. K. Singh (1993). Effect of Rotation on Unsteady Hydromagnetic Couette Flow. *Astrophys. Space Sci.* 202(1), 1-10.

Chauhan, D. S. and P. Rastogi (2012). Heat Transfer Effects on Rotating MHD Couette Flow in a Channel Partially Filled by a Porous Medium with Hall Current. *J. Appl. Sci. Eng.* 15(3), 281-290.

Chauhan, D. S. and R. Agrawal (2012). Effects of Hall Current on MHD Couette Flow in a Channel Partially Filled with a Porous Medium in a Rotating System. *Meccanica* 47(2), 405-421.

Cowling, T. G. (1957). *Magnetohydrodynamics*, Interscience Publishers, New York.

Cramer, K. R. and S. I. Pai (1973). *Magnetofluid Dynamics for Engineers and Applied Physicists*, McGraw Hill Book Company, New York.

Crepeau, J. C. and R. Clarksean, (1997). Similarity Solutions of Natural Convection with Internal Heat Generation, *J. Heat Transfer* 119, 183-185.

Das, S., S. L. Maji, M. Guria and R. N. Jana (2009). Unsteady MHD Couette Flow in a Rotating System. *Math. Computer Modelling* 50, 1211-1217.

Das, S., M. Jana and R. N. Jana (2011). Effects of Radiation on Free Convection Flow in a Vertical Channel Embedded in Porous Media. *Int. J. Computer Applications* 35(6), 38-44.

Datta, N. and R. N. Jana (1976). Effect of Wall Conductances on Hydromagnetic Convection of a Radiating Gas in a Vertical Channel. *Int. J. Heat Mass Transfer* 19(9), 1015-1019.

Delichatsios, M. A. (1988). *Air Entrainment into Buoyant Jet Flames and Pool Fires in DiNenno, P.J, et al*. (Eds.), The SFPA Handbook of Fire Protection Engineering, NFPA Publications, Quincy, M. A., 306-314.

Ghosh, S. K. (2002). Effects of Hall Current on MHD Couette Flow in a Rotating System with Arbitrary Magnetic Field. *Czech. J. Phys*. 52(1), 51-63.

Ghosh, S. K. and I. Pop (2004). Hall Effects on MHD Plasma Couette Flow in a Rotating Environment. *Int. J. Appl. Mech. Eng.* 9(2), 293-305.

Ghosh, S.K., O. A. Bég and M. Narahari (2013). A Study of Unsteady Rotating Hydromagnetic Free and Forced Convection in a Channel Subject to Forced Oscillation under an Oblique Magnetic Field. *J. Appl. Fluid Mech.* 6(2), 213-227.

Greif, R., I. S. Habib and J. C. Lin (1971). Laminar Convection of a Radiating Gas in a Vertical Channel. *J. Fluid Mech*. 46(3), 513-520.

Guchhait, S., S. Das, R. N. Jana and S. K. Ghosh (2011). Combined Effects of Hall Current and Rotation on Unsteady Couette Flow in a Porous Channel. *World J. Mech.* 1(3), 87-99.

Gupta, P. S. and A. S. Gupta (1974). Radiation Effect on Hydromagnetic Convection in a Vertical Channel. *Int. J. Heat Mass Transfer* 17(12), 1437-1442.

Haddad, O. H. (1999). Fully Developed Free Convection in Open-ended Vertical Channels Partially Filled with Porous Material. *J. Porous Med.* 2(2), 179-189.

Hayat, T., S. Nadeem and S. Asghar (2004a). Hydromagnetic Couette flow of an Oldroyd-B fluid in a rotating system. *Int. J. Eng. Sci.* 42(1), 65-78.

Hayat, T., S. Nadeem, A. M. Siddiqui and S. Asghar (2004b). An Oscillating Hydromagnetic Non-Newtonian Flow in a Rotating System. *Appl. Math. Lett.* 17(5), 609-614.

Hayat, T., K. Hutter, S. Nadeem and S. Asghar (2004c). Unsteady Hydromagnetic Rotating Flow of a Conducting Second Grade Fluid. *ZAMP* 55(4), 626-641.

Jana, R. N. and N. Datta (1980). Hall Effects on MHD Couette Flow in a Rotating System, *Czech. J. Phys.* 30, 659-667.

Jana, M., S. L. Maji, S. Das and R.N. Jana (2011). Convection of Radiating Gas in a Vertical Channel through Porous Media. *World J. Mech.* 1, 275-282.

Jana, M., S. L. Maji, S. Das, R. N. Jana and S. K. Ghosh (2014). Oscillatory Mixed Convection in a Porous Medium. *J. Appl. Fluid Mech*. 7(1), 43-50.

Jha, B. K. (2001). Natural Convection in Unsteady MHD Couette Flow. *Heat Mass Transfer* 37,329-331.

Jha, B. K. (2003). Transient Free-convective flow in a vertical channel with heat sink. *Int. J. Appl. Mech. Eng*. 8(3), 497-502.

Jha, B. K. and A. O. Ajibade (2009). Transient Natural Convection Flow between Vertical Parallel Plates with Temperature Dependent Heat Sources/Sinks. *Int J. Heat Tech.* 27(2), 87–94.

Jha, B. K. and A. O. Ajibade (2010). Unsteady Free Convective Couette Flow of Heat Generating/ Absorbing Fluid. *Int. J. Energy Tech.* 2(12), 1-9.

Jha, B. K. and C. A. Apere (2012). Time-dependent MHD Couette Flow of Rotating Fluid with Hall and Ion-slip Current. *Appl. Math. Mech*. 33(4), 399-410.

Joshi, H. M. (1988). Transient Effects in Natural Convection Cooling of Vertical Parallel Plates. *Int. Comm. Heat Mass Transfer*, 15(2), 227-238.

Kabakov, V. I. and Y. I. Yantovsky (1993). Solar Pond Magnetohydrodynamic Generator for Hydrogen Production. *Int. J. Hydrogen Energy* 18, 19-23.

Kim, S. H., N. K. Anand and W. Aung (1990). Effect of Wall Conduction on Free Convection between Asymmetrically Heated Vertical Plates: Uniform Wall Heat Flux. *Int. J. Heat Mass Transfer* 33(5), 1013-1023.

Lee, K. T. and W. M. Yan (1994). Laminar Natural Convection between Partially Heated Vertical Parallel Plates. *Heat Mass Transfer* 29, 145-

151.

Macheret, S. O., M. N. Shneider and R. B. Miles (2004). Magnetohydrodynamic and Electro-Hydrodynamic Control of Hypersonic Flows of Weakly Ionized Plasmas. *AIAA J.* 42, 10-19.

Mandal, C., S. Das and R. N. Jana (2012). Effect of Radiation on Transient Natural Convection Flow between Two Vertical Walls. *Int. J. Appl. Inform. Sys.* 2(2), 49-56.

Mckenzie, D. P., J. M. Roberts and N.O. Weiss, (1974). Convection in the Earth’s Mantle: Towards a Numerical Simulation, *J. Fluid. Mech*. 62, 465-538.

Meric, R. A. (1977). The Influences of a Magnetic Field on Free Convection in a Finite Vertical Channel. *Appl. Sci. Res.* 33, 459-469.

Miyatake, O. and T. Fujii (1972). Free Convection Heat Transfer between Vertical Plates- One Plate Isothermally Heated and other Thermally Insulated. *Heat Transfer-Japanese Res.* 3, 30-38.

Paul, T., B. K. Jha and A. K. Singh (1996). Transient Free Convective Flow in a Vertical Channel with Constant Temperature and Constant Heat Flux on Walls. *Heat Mass Transfer* 32, 61-63.

Sarkar, B.C., S. Das and R. N. Jana (2012). Oscillatory MHD Free Convective Flow between Two Vertical Walls in a Rotating System, *Adv. Appl. Sci. Res.* 3(5), 3311-3325.

Seth, G. S., R. N. Jana and M. K. Maiti (1982). Unsteady Hydromagnetic Couette Flow in a Rotating System. *Int. J. Eng. Sci*. 20(5), 989-999.

Seth, G. S., Md. S. Ansari and R. Nandkeolyar (2011). Effects of Rotation and Magnetic Field on Unsteady Couette Flow in a Porous Channel. *J. Appl. Fluid Mech.* 4(2), 95-103.

Seth, G. S., R. Nandkeolyar and Md. S. Ansari (2012). Effects of Hall Current and Rotation on Unsteady MHD Couette Flow in the Presence of an Inclined Magnetic Field. *J. Appl. Fluid Mech*. 5(2), 67-74.

Seth, G. S. and J. K. Singh (2013). Effects of Hall Current on Unsteady MHD Couette Flow of Class-II in a Rotating System, *J. Appl. Fluid Mech.* 6(4), 473-484.

Singh, A. K. (1988). Natural Convection in Unsteady Couette Motion, *Def. Sci. J.* 38(1), 35-41.

Singh, A. K., N. C. Sacheti and P. Chandran (1994). Transient Effects on Magnetohydrodynamic Couette Flow with Rotation: Accelerated Motion. *Int. J. Eng. Sci*. 32(1), 133-139.

Singh, A. K., H. R. Gholami and V. M. Soundalgekar (1996). Transient Free Convection Flow between Two Vertical Parallel Plates. *Heat Mass Transfer* 31(5), 329-331.

Singh, K. D. and R. Kumar (2010). An Exact Solution of an Oscillatory MHD Flow through a Porous Medium Bounded by Rotating Porous Channel in the Presence of Hall Current. *Int. J. Appl. Math. Mech.* 6(13), 28-40.

Vajravelu, K. and J. Nayfeh (1992). Hydromagnetic Convection at a Cone and a Wedge. *Int. Comm. Heat Mass Transfer* 19, 701-710.

Vogin, C., and A. Alemany (2007). Analysis of the Flow in a Thermo-acoustic MHD Generator with Conducting Walls. *Eur. J. Mech. - B/Fluids* 26(4), 479-493.

Weidman, P. D. and A. Medina (2008). Porous Media Convection between Vertical Walls: Continuum of Solutions from Capped to Open Ends. *Acta Mech.* 199, 209-216.

Westphal, B. R., D. D. Keiser, R. H. Rigg and D. V. Loug (1994). Production of Metal Waste Forms From Spent Nuclear Fuel Treatment, *Proc. DOE Spent Nucl. Fuel Confer., Salt Lake City, UT* 288-294.

Yamasaki, H., S. Kabashima, S. Shioda and Y. Okuno (1988). Unsteady Discharge and Fluid Flow in a Closed-Cycle Disk MHD Generator. *AIAA J. Propulsion Power* 4(1), 61-67.

Yu, C. P. (1965). Combined Forced and Free Convection Channel Flows in Magneto-hydrodynamics. *AIAA J*. 3(6), 1184-1186.

Zueco, J., O. A. Bég , H. S. Takhar and V. R. Prasad (2009). Thermophoretic Hydromagnetic Dissipative Heat and Mass Transfer with Lateral Mass Flux, Heat Source, Ohmic Heating and Thermal Conductivity Effects: Network Simulation Numerical Study. *Appl. Therm. Eng.* 29, 2808-2815.

APPENDIX-I

$\alpha_1 = a\sqrt{P_r\varphi}$, $\alpha_2 = b\sqrt{P_r\varphi}$, $\alpha_3 = a\sqrt{\lambda_1}$, $\alpha_4 = b\sqrt{\lambda_1}$,
$\alpha_5 = a\sqrt{\lambda_1+\lambda_2}$, $\alpha_6 = b\sqrt{\lambda_1+\lambda_2}$, $\alpha_7 = a\sqrt{P_r(\varphi+\lambda_2)}$,
$\alpha_8 = b\sqrt{P_r(\varphi+\lambda_2)}$,
$\beta_1 = a\sqrt{P_r/t}/2$, $\beta_2 = b\sqrt{P_r/t}/2$, $\beta_3 = a/2\sqrt{t}$,
$\beta_4 = b/2\sqrt{t}$,
$\gamma_1 = \sqrt{\varphi t}$, $\gamma_2 = \sqrt{\lambda_1 t}$, $\gamma_3 = \sqrt{(\lambda_1+\lambda_2)t}$,
$\gamma_4 = \sqrt{(\varphi+\lambda_2)t}$,
$a = 2k+\eta, \quad b = 2+2k-\eta.$

APPENDIX-II

$$\theta_1(k) = e^{2k\sqrt{\lambda_1}} erfc\left(k/\sqrt{t} + \sqrt{\lambda_1 t}\right),$$

$$\theta_2(k) = e^{-2k\sqrt{\lambda_1}} erfc\left(k/\sqrt{t} - \sqrt{\lambda_1 t}\right),$$

$$\theta_3(k) = e^{2k\sqrt{\lambda_1+\lambda_2}} erfc\left(k/\sqrt{t} + \sqrt{(\lambda_1+\lambda_2)t}\right),$$

$$\theta_4(k) = e^{-2k\sqrt{\lambda_1+\lambda_2}} erfc\left(k/\sqrt{t} - \sqrt{(\lambda_1+\lambda_2)t}\right),$$

$$\theta_5(k) = e^{2k\sqrt{P_r(\varphi+\lambda_2)}} erfc\left(k\sqrt{P_r/t} + \sqrt{(\varphi+\lambda_2)t}\right),$$

$$\theta_6(k) = e^{-2k\sqrt{P_r(\varphi+\lambda_2)}} erfc\left(k\sqrt{P_r/t} - \sqrt{(\varphi+\lambda_2)t}\right),$$

$$\theta_7(k) = e^{2k\sqrt{P_r\varphi}} erfc\left(k\sqrt{P_r/t} + \sqrt{\varphi t}\right),$$

$$\theta_8(k) = e^{-2k\sqrt{P_r\varphi}} erfc\left(k\sqrt{P_r/t} - \sqrt{\varphi t}\right),$$

$$\psi_1(k) = e^{-\left(\frac{k^2}{t}+\lambda_1 t\right)}, \qquad \psi_2(k) = e^{-\left(\frac{k^2}{t}+(\lambda_1+\lambda_2)t\right)},$$

$$\psi_3(k) = e^{-\left(\frac{k^2P_r}{t}+(\varphi+\lambda_2)t\right)}, \qquad \psi_4(k) = e^{-\left(\frac{k^2P_r}{t}+\varphi t\right)}.$$

APPENDIX-III

$$\varphi_1 = \frac{ae^{-a^2/4t}}{\xi_1}\sqrt{\frac{1}{\pi t}}\left[\left(a^2/4t - m_1 t\right)\cos(m_2 t) + m_2 t\sin(m_2 t)\right],$$

$$\varphi_2 = \frac{ae^{-a^2/4t}}{\xi_1}\sqrt{\frac{1}{\pi t}}\left[\left(a^2/4t - m_1 t\right)\sin(m_2 t) - m_2 t\cos(m_2 t)\right],$$

$$\varphi_3 = \frac{be^{-b^2/4t}}{\xi_2}\sqrt{\frac{1}{\pi t}}\left[\left(b^2/4t - m_1 t\right)\cos(m_2 t) + m_2 t\sin(m_2 t)\right],$$

$$\varphi_4 = \frac{be^{-b^2/4t}}{\xi_2}\sqrt{\frac{1}{\pi t}}\left[\left(b^2/4t - m_1 t\right)\sin(m_2 t) - m_2 t\cos(m_2 t)\right],$$

$$\varphi_5 = \frac{ae^{-a^2P_r/4t}}{\xi_3}\sqrt{\frac{P_r}{\pi t}}\left[\left(a^2P_r/4t - m_7 t\right)\cos(m_6 t) + m_6 t\sin(m_6 t)\right],$$

$$\varphi_6 = \frac{ae^{-a^2P_r/4t}}{\xi_3}\sqrt{\frac{P_r}{\pi t}}\left[\left(a^2P_r/4t - m_7 t\right)\sin(m_6 t) - m_6 t\cos(m_6 t)\right],$$

$$\varphi_7 = \frac{be^{-b^2P_r/4t}}{\xi_4}\sqrt{\frac{P_r}{\pi t}}\left[\left(b^2P_r/4t - m_7 t\right)\cos(m_6 t) + m_6 t\sin(m_6 t)\right],$$

$$\varphi_8 = \frac{be^{-b^2P_r/4t}}{\xi_4}\sqrt{\frac{P_r}{\pi t}}\left[\left(b^2P_r/4t - m_7 t\right)\sin(m_6 t) - m_6 t\cos(m_6 t)\right],$$

$$\varphi_9 = \frac{ae^{-a^2/4t}}{\xi_5}\sqrt{\frac{1}{\pi t}}\left[\left(a^2/4t - m_3 t\right)\cos(m_4 t) + m_4 t\sin(m_4 t)\right],$$

$$\varphi_{10} = \frac{ae^{-a^2/4t}}{\xi_5}\sqrt{\frac{1}{\pi t}}\left[\left(a^2/4t - m_3 t\right)\sin(m_4 t) - m_4 t\cos(m_4 t)\right],$$

$$\varphi_{11} = \frac{be^{-b^2/4t}}{\xi_6}\sqrt{\frac{1}{\pi t}}\left[\left(b^2/4t - m_3 t\right)\cos(m_4 t) + m_4 t\sin(m_4 t)\right],$$

$$\varphi_{12} = \frac{be^{-b^2/4t}}{\xi_6}\sqrt{\frac{1}{\pi t}}\left[\left(b^2/4t - m_3 t\right)\sin(m_4 t) - m_4 t\cos(m_4 t)\right],$$

$$\varphi_{13} = \frac{ae^{-a^2P_r/4t}}{\left(a^2P_r/4t - \varphi t\right)}\sqrt{\frac{P_r}{\pi t}},$$

$$\varphi_{14} = \frac{be^{-b^2P_r/4t}}{\left(b^2P_r/4t - \varphi t\right)}\sqrt{\frac{P_r}{\pi t}},$$

$$\xi_1 = \left(a^2/4t - m_1 t\right)^2 + m_2^2 t^2, \qquad \xi_2 = \left(b^2/4t - m_1 t\right)^2 + m_2^2 t^2,$$

$$\xi_3 = \left(a^2P_r/4t - m_7 t\right)^2 + m_6^2 t^2, \quad \xi_4 = \left(b^2P_r/4t - m_7 t\right)^2 + m_6^2 t^2,$$

$$\xi_5 = \left(a^2/4t - m_3 t\right)^2 + m_4^2 t^2, \qquad \xi_6 = \left(b^2/4t - m_3 t\right)^2 + m_4^2 t^2.$$